九州大学学術情報リポジトリ
Kyushu University Institutional Repository

DOCK8 controls survival of group 3 innate lymphoid cells in the gut through Cdc42 activation

Aihara, Ryosuke
Division of Immunogenetics, Department of Immunobiology and Neuroscience, Medical Institute of Bioregulation, Kyushu University

Kunimura, Kazufumi
Division of Immunogenetics, Department of Immunobiology and Neuroscience, Medical Institute of Bioregulation, Kyushu University

Watanabe, Mayuki
Division of Immunogenetics, Department of Immunobiology and Neuroscience, Medical Institute of Bioregulation, Kyushu University

宇留野, 武人
Division of Immunogenetics, Department of Immunobiology and Neuroscience, Medical Institute of Bioregulation, Kyushu University

他

https://hdl.handle.net/2324/4495853

出版情報：International immunology. 33 (3), pp.149-160, 2020-09-28. Oxford University Press
バージョン：
権利関係：

KYUSHU UNIVERSITY

DOCK8 controls survival of group 3 innate lymphoid cells in the gut through Cdc42 activation

Ryosuke Aihara[1,2]†, **Kazufumi Kunimura**[1]†*, **Mayuki Watanabe**[1,3], **Takehito Uruno**[1], **Nana Yamane**[1], **Tetsuya Sakurai**[1], **Daiji Sakata**[1], **Fusanori Nishimura**[2] and **Yoshinori Fukui**[1]*

[1]Division of Immunogenetics, Department of Immunobiology and Neuroscience, Medical Institute of Bioregulation, Kyushu University, 3-1-1 Maidashi, Higashi-ku, Fukuoka 812-8582, Japan

[2]Section of Periodontology, Division of Oral Rehabilitation, Faculty of Dental Science, Kyushu University, 3-1-1 Maidashi, Higashi-ku, Fukuoka 812-8582, Japan

†These authors contributed equally to this work.

[3]Present address: Japan Agency for Medical Research and Development, Tokyo 100-0004, Japan

**Correspondence to:* Y. Fukui; E-mail: fukui@bioreg.kyushu-u.ac.jp or K. Kunimura; E-mail: kunimura@bioreg.kyushu-u.ac.jp

Keywords: ILC3s, IL-22, Rho family of GTPases, survival

Abstract

Innate lymphoid cells (ILCs) are a family of developmentally related leukocytes that rapidly secrete polarized sets of cytokines to combat infection and promote tissue repair at mucosal barriers. Among them, group 3 ILCs (ILC3s) play an important role in maintenance of the gut homeostasis by producing interleukin 22 (IL-22), and their development and function critically depend on the transcription factor RORγt. Although recent evidence indicates that RORγt$^+$ ILC3s are reduced in the gut in the absence of the Cdc42 activator DOCK8 (dedicator of cytokinesis 8), the underlying mechanism remains unclear. We found that genetic deletion of *Dock8* in RORγt$^+$-lineage cells markedly reduced ILC3s in the lamina propria of the small intestine. By analyzing BrdU incorporation, it was revealed that DOCK8 deficiency did not affect the cell proliferation. Furthermore, when lineage marker-negative (Lin$^-$) α4β7$^+$ CD127$^+$ RORγt$^-$ fetal liver cells were cultured with OP9 stromal cells in the presence of stem cell factor (SCF) and IL-7 *in vitro*, RORγt$^+$ ILC3s normally developed irrespective of DOCK8 expression. However, DOCK8-deficient ILC3s exhibited a severe defect in survival of ILC3s under the condition with or without IL-7. Similar defects were observed when we analyzed *Dock8*^{VAGR} mice having mutations in the catalytic center of DOCK8, thereby failing to activate Cdc42. Thus, DOCK8 acts in cell-autonomous manner to control survival of ILC3s in the gut through Cdc42 activation.

Introduction

Innate lymphoid cells (ILCs) are a family of developmentally related leukocytes that are involved in protective immunity and tissue remodeling (1). They are classified into three groups on the basis of their requirement of transcription factors and production of the effector cytokines (2). Group 1 ILCs (ILC1s) require T-bet and produce interferon-γ (IFN-γ), and group 2 ILCs (ILC2s) produce interleukin 5 (IL-5) and IL-13 depending on GATA-3 and RORα (3). On the other hand, group 3 ILCs (ILC3s) express RORγt and produce IL-22, which promotes repair of the intestinal epithelial cells and induce secretion of antimicrobial peptides (4). Therefore, IL-22-producing ILC3s play a key role in maintenance of the gut homeostasis. ILC3s are further subdivided into at least three subsets such as NKp46^{+} ILC3s, CD4^{+} ILC3s, and NKp46^{-} CD4^{-} double-negative ILC3s (DN-ILC3s) (5). NKp46^{+} ILC3s are especially important for mucosal defense against infections and abundantly found in the intestinal lamina propria, whereas CD4^{+} ILC3s mainly localize to cryptopatches (CPs) and isolated lymphoid follicles (ILFs) (6). CD4^{+} ILC3s include lymphoid tissue inducer cells (LTi cells) in fetuses and LTi-like cells in adults, both of which play a unique role in the development of secondary lymphoid organs, such as CPs and ILFs (6–8).

Cdc42 is a member of the small GTPases that function as molecular switches by cycling between GDP-bound inactive and GTP-bound active states (9). The stimulus-induced formation of active Cdc42 is mediated by guanine nucleotide exchange factors (GEFs), and once activated, Cdc42 binds to multiple effector molecules (10). Cdc42 is known to act as a master regulator of cell polarity in eukaryotic organisms ranging from yeasts to humans (10). However, recent evidence indicates that Cdc42 is involved in many physiological functions than

previously thought. For example, Cdc42-deficient dendritic cells (DCs) fail to migrate effectively within 3-dimensional (3D) extracellular matrix scaffolds (11), and Cdc42-deficient neutrophils exhibit defects in bacterial killing and phagocytic endocytosis (12). In addition, genetic deletion of Cdc42 in B cells and T cells impairs their proliferation and survival (13, 14). Thus, Cdc42 plays important roles in migration and functions of leukocytes.

Dedicator of cytokinesis 8 (DOCK8) is a member of the evolutionarily conserved DOCK family proteins that functions as GEFs for the Rho family of GTPases (15). DOCK8 interacts with Cdc42 and mediates the GTP-GDP exchange reaction through the DOCK homology region 2 (DHR2) domain (16). Recently, much attention has been paid to the signaling and functions of DOCK8, because it has been reported that the bi-allelic *DOCK8* mutations in humans cause a combined immunodeficiency characterized by severe/persistent cutaneous viral infections, early-onset malignancy, and atopic dermatitis (17–20). Accumulating evidence indicates that human patients with *DOCK8* mutations have morphological and functional abnormalities of leukocytes (19, 21–24). In addition, the important roles of DOCK8 in leukocytes have been demonstrated using animal models. For example, *N*-ethyl-*N*-nitrosourea–mediated mutagenesis in mice has shown that DOCK8 regulates immunological synapse formation in B cells and is required for development or survival of memory $CD8^+$ T cells and natural killer T cells (23–27). Interestingly, these mice exhibited a reduction of ILC3s in the small intestine (28). However, the underlying mechanism is not completely understood.

In this study, we found that genetic deletion of *Dock8* in $ROR\gamma t^+$-lineage cells markedly reduced ILC3s in the lamina propria of the small intestine. Further investigation showed that the survival of ILC3s was impaired in both conventional

DOCK8-deficient (*Dock8*$^{-/-}$) mice and *Dock8*^{VAGR} mice having point mutations in the catalytic center of DOCK8, thereby failing to activate Cdc42. Thus, our results indicate that DOCK8 acts in cell-autonomous manner to regulate the survival of ILC3s in the gut through Cdc42 activation.

Methods

Mice

DOCK8-deficient (*Dock8*$^{-/-}$) mice have been previously described (16). *Dock8*$^{-/-}$ mice were backcrossed onto a C57BL/6J background for more than 9 generations prior to analyses. *Dock8*$^{lox/lox}$ mice (29), BAC-transgenic RORγt-GFP Tg mice (30), *Rorc-Cre* Tg mice (30) and *CD11c (Itgax)-Cre* Tg mice (31) have been previously described. *Dock8*^{VAGR} knock-in mutant mice (V1986A / G1980R) were generated by using CRISPR/Cas9-mediated genome editing system as described below (Supplementary Figure 1). Male and female mice were used at 8-12 weeks of age, and age-matched littermate mice were used as controls. To isolate fetal liver cells, fetus was collected on embryonic day 14.5 (E14.5). Mice were maintained in specific pathogen-free conditions in the animal facility of Kyushu University. All experiments were conducted in accordance with the guidelines of the Committee of Ethics of Animal Experiments in Kyushu University.

Generation of Dock8^{VAGR} mice

A custom-designed DOCK8 locus-specific CRISPR RNA (5'-<u>ATGCTGCAAATG GTACTGCA</u>GUUUUAGAGCUAUGCU-3'; the target guide RNA sequence underlined) was made into a duplex with the generic tracer RNA (Integrated DNA Technologies, Coralville, IA, USA). Sixty pmole of the duplex guide RNA was incubated with 6 ng of Cas9-3NLS protein (Integrated DNA Technologies) in 1x Opti-MEM (Thermo Fisher Scientific, Waltham, MA, USA) for 10 min at room temperature to form a Cas9-guide RNA (RNP: ribonucleoprotein) complex, then followed by addition of 180 pmole of single-stranded donor oligonucleotides (ssODN; 5'-CATCACCTCCTAAGAGTAGAGACCACGTAAACAAACAAGCCCTAA

CCAAGCTGCCATTAGTGAGCCCAGCTTACCTGATTTGCAGTGGCTCCTACAGA GCGCTGCAGTACCATTTGCAGCATCTTTGCATCAGGGGGCTCCTGGTGAGTG GCCACGGCTAACTGCAGGGTCTTCTTCTTC-3'; mutated positions underlined) as a template for homology-directed DNA repair. Mouse pronuclear-stage embryos were obtained by the standard *in vitro* fertilization method from C57BL/6J donors (CLEA Japan, Tokyo, Japan). At 7 h from insemination, the Cas9 RNP complex and donor oligo were transferred to intact pronuclear-stage embryos using NEPA 21 super electroporator and 5-mm gap platinum metal electrode (NEPA Gene, Chiba, Japan). Setting parameters were as follows; Poring pulse: Voltage 225 V, Pulse length 2 milli-sec, Pulse interval 50 milli-sec, Number of pulses +4, Decay rate 10%. Transfer pulse: Voltage 20 V, Pulse length 50 milli-sec, Pulse interval 50 milli-sec, Number of pulses ± 5, Decay rate 40%. The embryos were cultured overnight, and 2-cell stage embryos were selected and transferred to ICR host females. To identify correctly targeted offspring, the target *Dock8* locus was amplified by PCR, and cloned by TA cloning. After verifying their sequence, the founder *Dock8*^{VAGR} male mouse was crossed with C57BL/6J female mouse to obtain mice that successfully transmitted the mutated allele.

Reagents

Paraformaldehyde (PFA), phorbol 12-myristate 13-acetate (PMA), ionomycin calcium salt, and brefeldin A were purchased from Sigma-Aldrich (St Louis, MO, USA). Periodate–lysine-paraformaldehyde (PLP) Solution Set was purchased from Wako (Osaka, Japan).

Isolation of immune cells

Intestinal lamina propria cells were extracted from the small intestine as described previously (32). Briefly, after removal of the Peyer's patches, the small intestines were washed with PBS and cut into small pieces. They were incubated with PBS containing 3 mM EDTA for 15 min and RPMI-1640 medium (Wako) containing 1% fetal calf serum (FCS) (Thermo Fisher Scientific), 1% penicillin-streptomycin (Thermo Fisher Scientific), 1 mM EGTA, and 2 mM $MgCl_2$ for 20 min each repeatedly twice to remove epithelial cells. Lamina propria cells were isolated by digestion with 200 U ml^{-1} collagenase (Wako) and 5 μg ml^{-1} DNaseI (Roche, Basel, Switzerland) for 60 min at 37°C. After homogenized, cell suspensions were additionally incubated for 30 min, and then purified by 45%/66% Percoll (GE Healthcare, Uppsala, Sweden) gradient. Fetal livers were mechanically dissociated through 70-μm filters and resuspended in HBSS (Thermo Fisher Scientific) containing 0.25% BSA (Sigma-Aldrich) and 5 mM sodium azide (Sigma-Aldrich).

Flow cytometry and cell sorting

Before staining with antibodies, cells were incubated for 10 min on ice with anti-mouse CD16/32 (Fcγ III/II receptor; 2.4G2, 1:1000, BD Biosciences) to block Fc receptors. Cells were then stained with the following antibodies: FITC- or PerCP-Cyanine 5.5-conjugated anti-mouse CD3ε (1:100, 145-2c11, TONBO biosciences, CA, USA), biotinylated anti-mouse CD3ε (1:200, 145-2c11, BD Biosciences), FITC-conjugated anti-mouse B220 (1:100, RA3-6B2, TONBO biosciences), biotinylated anti-mouse B220 (1:200, RA3-6B2, BD Biosciences), FITC-conjugated anti-mouse CD8α (1:100, 53-6.7, TONBO biosciences), biotinylated anti-mouse CD8α (1:200, 53-6.7, BD Biosciences), FITC-conjugated anti-mouse CD11b (1:100, M1/70, TONBO biosciences), biotinylated anti-mouse

CD11b (1:200, M1/70, BD Biosciences), PE-conjugated anti-mouse CD11b (1:200, M1/70, BD Biosciences), FITC-conjugated anti-mouse CD11c (1:100, HL3, BD Biosciences), biotinylated anti-mouse CD11c (1:200, HL3, BD Biosciences), FITC-conjugated anti-mouse Ly6G/Ly6C (1:100, RB6-8C5, TONBO biosciences), biotinylated anti-mouse Ly6G/Ly6C (1:200, RB6-8C5, BD Biosciences), FITC-conjugated anti-mouse FcεR1 (1:100, MAR-1, TONBO biosciences), biotinylated anti-mouse FcεR1 (1:200, MAR-1, eBioscience, San Diego, CA, USA), FITC-conjugated anti-mouse NK1.1 (1:100, PK136, TONBO biosciences), biotinylated anti-mouse NK1.1 (1:200, PK136, BioLegend, CA, USA), PE-conjugated anti-mouse Sca-1 (1:100, D7, BD Biosciences), PE-conjugated anti-mouse NKp46 (1:100, 29A1.4, BD Biosciences), biotinylated anti-mouse NKp46 (1:200, 29A1.4, eBioscience), APC-conjugated anti-mouse CD127 (1:100, A7R34, BioLegend), PE-conjugated anti-mouse CD19 (1:100, 1D3, TONBO biosciences) , PerCP-eFluor 710-conjugated anti-human/mouse IL-22 (1:50, IL22JOP, eBioscience), APC-conjugated anti-mouse RORγt (1:50, B2D, eBioscience), biotinylated anti-mouse c-Kit (1:100, 2B8, BD Biosciences), biotinylated anti-mouse α4β7 (1:200, DATK32, TONBO biosciences) followed by incubation with PerCP-conjugated streptavidin (1:500, BioLegend). Intracellular cytokine staining of immune cells was performed with a Cytofix/Cytoperm Plus Kit (BD Biosciences) after stimulation with 50 ng ml^{-1} PMA and 500 ng ml^{-1} ionomycin calcium salt at 37°C for 4 h in the presence of 10 μg ml^{-1} Brefeldin A. RORγt expression in immune cells was analyzed with a Transcription Factor Buffer Set (eBioscience). To analyse DOCK8 expression, intestinal ILC3s were sorted as RORγt-$GFP^{+}$$Lineage^{-}$ (CD3ε, B220, CD8α, CD11b, CD11c, Ly6G/Ly6C, FcεR1, NK1.1) cells. As controls, splenic B cells ($CD19^{+}CD3\varepsilon^{-}$ cells), bone marrow (BM)

neutrophils (Ly6G/Ly6C$^+$CD11b$^+$ cells), and intestinal T cells (CD3ε^+ cells in the lamina propria) were sorted. Flow cytometric analyses or sorting was performed with BD FACSVerse or BD FACSAria II (BD Biosciences), respectively. The sorted cells (intestinal ILC3s, BM neutrophils, splenic B cells and intestinal T cells) were of at least 95% purity. Data analysis was performed using BD FACSuite software (BD Biosciences).

Immunohistochemistry

After the Peyer's patches were dissected, the small intestines were fixed in 1% periodate–lysine-paraformaldehyde (PLP) (Wako) overnight at 4°C. Then, fixed tissues were incubated overnight with 30% sucrose in PBS at 4°C, and embedded in OCT compound (Sakura Finetech, Tokyo, Japan). After being frozen at –80°C, cryostat sections (5 μm thick) were blocked with 1% bovine serum albumin (BSA) (Sigma-Aldrich) in PBS containing 0.1% Tween-20 (Wako) for 1 h at room temperature and stained with following antibodies: APC-conjugated anti-mouse CD3ε (1:200, 145-2c11, TONBO biosciences), PE-conjugated anti-mouse B220 (1:200, RA3-6B2, TONBO biosciences), and DAPI solution (1:5000, Dojindo Laboratories, Kumamoto, Japan). GFP expression in RORγt-GFP Tg mice was visualized with Alexa Fluor 488-conjugated polyclonal anti-GFP antibody (1:100, Invitrogen, Carlsbad, CA, USA). Images were obtained with a laser scanning confocal microscope (FV3000; Olympus, Tokyo, Japan). The number of cryptopatches (CPs; RORγt$^+$B220$^-$ clusters) and isolated lymphoid follicles (ILFs; RORγt$^+$B220$^+$ clusters) was counted manually in 20 sections of 6 cm length.

Whole-mount immunostaining

Mice were treated intraperitoneally (i.p.) with recombinant murine IL-22 (1 μg, Peprotech) or PBS as a control one day before analysis. Immunofluorescent staining for fucosylation of epithelial cells was performed as described (33). The mucus layer was removed from small intestines with PBS followed by fixation with 4% paraformaldehyde for 4 h. After washing twice with PBS, whole-mount tissues were stained with biotinylated anti-ulex europaeus agglutinin-1 (UEA-1) (1:200, Vector Laboratories, Burlingame, CA, USA) and anti-wheat germ agglutinin (WGA) conjugated to Alexa Fluor 488 (1:200, Invitrogen) overnight at 4°C. Streptavidin-Alexa Fluor 546 (1:400, Invitrogen) was used as a secondary antibody to detect the biotinylated primary antibody. Samples were then stained with DAPI solution (1:5000, Dojindo Laboratories) for 5 min. All images were obtained with a laser scanning confocal microscope (FV3000; Olympus).

Reverse transcription-PCR

Total RNA was extracted from the sorted cells (intestinal ILC3s, bone marrow neutrophils, splenic B cells, and intestinal T cells) with ISOGEN (Nippon Gene, Tokyo, Japan). After treatment with RNase-free DNase I (Thermo Fisher Scientific), RNA samples were reverse-transcribed with Oligo$(dT)_{12\text{-}18}$ primers (Thermo Fisher Scientific) and SuperScript III reverse transcriptase (Thermo Fisher Scientific) for amplification by PCR. For conventional reverse transcription-PCR, the following PCR primers were used: *Gapdh,* 5'-CCCATCACCATCTTCCAG-3' and 5'-ATGACCTTGCCCACAGCC -3'; *Dock8*, 5'-TGGCCTTCACACCCAAAGAA-3' and 5'-GAACACAGTCTCTGACGTGAGG-3'.

Culture of fetal liver cells

All experiments were performed in RPMI 1640 medium containing 10% heat-inactivated fetal calf serum (FCS), 50 μM 2-mercaptoethanol (Nacalai tesque, Kyoto, Japan), 2 mM L-glutamine (Thermo Fisher Scientific), 100 U ml^{-1} penicillin (Thermo Fisher Scientific), 100 μg ml^{-1} streptomycin (Thermo Fisher Scientific), 1 mM sodium pyruvate (Thermo Fisher Scientific), and 1 x MEM non-essential amino acids (Thermo Fisher Scientific) (designated complete RPMI medium). Fetal liver cell culture was performed as previously described (34), with some modifications. Before experiments, OP9 stromal cells (1 x 10^3) were plated at 70% confluency onto 96-well plates and irradiated (15 Gy). Fetal liver cells were incubated with biotinylated antibodies to the following lineage markers (CD3ε, B220, CD8α, CD11b, CD11c, Ly6G/Ly6C, FcεR1, NK1.1), and lineage marker-positive cells were depleted using streptavidin-conjugated microbeads (Miltenyi Biotec, Auburn, CA, USA) and the MACS Separators (Miltenyi Biotec). Then, lineage marker-negative (Lin^-) $\alpha4\beta7^+CD127^+ROR\gamma t\text{-}GFP^-$ cells (1–8 x 10^3) were sorted with FACSAria II (BD Biosciences) and plated on irradiated OP9 stromal cells in complete RPMI medium containing 25 ng ml^{-1} murine IL-7 (Peprotech, Rocky Hill, NJ, USA) and 25 ng ml^{-1} murine stem cell factor (SCF) (Peprotech). Cells were maintained in a 37°C incubator (Thermo Fisher Scientific) with 5% CO_2 and analyzed after 7 days of culture.

BrdU-incorporation assay

The BrdU-incorporation assay has been described previously (35). Briefly, mice were injected i.p. with BrdU (200 μg, BD Biosciences) and recombinant murine IL-23 (1 μg, Peprotech), and then fed continuously with water containing 800 μg ml^{-1} BrdU and 5% glucose for 16 h. $BrdU^+$ ILC3s ($Lin^-ROR\gamma t\text{-}GFP^+$) in the lamina propria

of the small intestine were analyzed by BD FACSVerse (BD Biosciences) with APC BrdU Flow Kit (BD Biosciences) in accordance with the manufacturer's instructions.

In vitro apoptosis assay

The Annexin V expression on ILC3s was analyzed as described previously (36). Briefly, we sorted ILC3s ($Lin^{-}ROR\gamma t\text{-}GFP^{+}$) into V-bottom 96-well plates and cultured them with or without 25 ng ml^{-1} murine IL-7 for 18 h. Then, cell apoptosis was examined by staining ILC3s with APC-Annexin V or PE-Annexin V (1:20, BD Biosciences) in accordance with the manufacturer's instructions.

Plasmids and transfection

The genes encoding DOCK8 and its mutants with appropriate tags were created by PCR, and subcloned into the pcDNA (Invitrogen) vector. These plasmids were transfected into HEK-293T cells with polyethylenimine (Sigma-Aldrich).

Pull-down assay

HEK-293T cells expressing hemagglutinin (HA)-tagged DOCK8 (Wild type, V1986A mutation, G1980R mutation, V1986A / G1980R mutations) were lysed by adding 1 x Mg^{2+} lysis buffer (MLB; 25 mM HEPES (pH 7.5), 150 mM NaCl, 1% Igepal CA-630, 10 mM $MgCl_2$, 1 mM EDTA, and 10% glycerol; EMD Millipore, Burlington, MA, USA), followed by centrifugation at 20,000*g* for 1 min at 4°C. Aliquots were saved for total cell lysate controls, and the remaining lysates were incubated with agarose beads containing the GST-fusion Cdc42-binding domain of PAK1 (EMD Millipore) at 4°C for 1 h. The beads were washed twice with 1 x MLB buffer and suspended in SDS-PAGE sample buffer (62.5 mM tris-HCl (pH 6.8), 2% SDS, 10% glycerol,

0.005% bromophenol blue, and 2.5% 2-mercaptoethanol). The bound proteins and the total cell lysates were separated by SDS-PAGE on a 12.5% or 7.5% polyacrylamide gel, and the blots were probed with rat anti-HA antibody (1:1000, Roche) or mouse anti-Cdc42 antibody (1:1000, BD Biosciences).

In vitro GEF assay

The GEF assay was performed as previously described (37). Briefly, the genes encoding the DOCK8-DHR2 domain, and its mutant were expressed in *E. coli* Arctic Express (Stratagene, La Jolla, CA, USA) as fusion proteins with the His-SUMO tag at their N termini for purification with nickel-nitrilotriacetic acid-agarose chromatography (Qiagen, Hilden, NRW, Germany). The GST fusion Cdc42 and GST alone were expressed in BL21 (Agilent Technologies, Santa Clara, CA, USA), and purified on glutathione-Sepharose™ 4B (GE Healthcare) immediately before use. The assays consisted of GST fusion Cdc42 (10 μM), BODIPY-FL GTP (2.4 μM, Invitrogen), and the His-SUMO tagged recombinant WT DOCK8-DHR2 domain (residues 1633–2071) or its VA, GR, and VAGR mutants (specified concentrations) in reaction buffer (20 mM MES-NaOH, 150 mM NaCl, 10 mM MgCl2, and 20 μM GDP (pH 7.0)). For this purpose, GST fusion Cdc42 (15.56 μM) was loaded with GDP by incubation in reaction buffer in a total volume of 96.4 μl on ice for 30 min, and mixed with BODIPY-FL GTP (0.1 mM, 3.6 μl), and then allowed to equilibrate at 30°C for 3 min. Recombinant DOCK8-DHR2 protein was equilibrated in reaction buffer in a total volume of 50 μl for 30 min at room temperature. The reaction was initiated by mixing GDP-loaded Cdc42/BODIPY-FL GTP (100 μl) and the recombinant DOCK8-DHR2 domain (50 μl) in a final volume of 150 μl and incubating at 30°C. The change in the BODIPY-FL-GTP fluorescence (excitation;

488 nm, emission; 514 nm) was monitored for 20 min using an EnSpire multimode plate reader (PerkinElmer, Waltham, MA, USA). Data were fitted using the curve fitting function in the GraphPad Prism 7.0 software program (GraphPad Software, San Diego, CA, USA), and the initial slope during the first 10 s (in relative fluorescence units [RFU] per second) was calculated and used for comparison of the GEF activity.

Statistical analysis

Statistical analyses were performed using Prism 7.0 (GraphPad Software). The data was initially tested with a Kolmogorov-Smirnov test for normal distribution. Parametric data were analyzed using a two-tailed unpaired Student's *t*-test when two groups were compared. *P*-values less than 0.05 were considered significant.

Results

Reduction of ILC3s in the small intestine in the absence of DOCK8

ILC3s are the heterogeneous cell population and can be subdivided into at least three different groups, each of which is characterized by the expression of CD4 and NKp46 (5). To determine the role of DOCK8 in ILC3s, we first compared the percentage and the number of ILC3s in the intestinal lamina propria between *Dock8*$^{+/-}$ and *Dock8*$^{-/-}$ mice under the steady state. We found that the percentage of both NKp46^{+} ILC3s (Lin^{-}NKp46^{+}RORγt^{+}) and CD4^{+} ILC3s (Lin^{-}CD4^{+}RORγt^{+}) in total Lin^{-} populations significantly reduced in *Dock8*$^{-/-}$ mice (Fig. 1A, middle). Similar results were obtained when the absolute number of these ILC3 subsets were compared between *Dock8*$^{+/-}$ and *Dock8*$^{-/-}$ mice (Fig. 1A, right). This was further confirmed by flow cytometric analysis of the intestinal lamina propria in *Dock8*$^{+/-}$ and *Dock8*$^{-/-}$ mice expressing GFP under the control of the mouse *Rorc* promoter (RORγt-GFP mice) (Fig. 1B). Immunofluorescence staining also revealed that the numbers of CPs (RORγt^{+}B220^{-} clusters) and ILFs (RORγt^{+}B220^{+} clusters) containing large amounts of ILC3s were notably reduced in *Dock8*$^{-/-}$ mice as compared with that in *Dock8*$^{+/-}$ mice (Fig. 1C).

It is known that ILC3s produce large amounts of IL-22, which are critical for the induction and regulation of epithelial fucosylation contributing to protective immunity against enteric pathogens, such as *Salmonella typhimurium* (33). Therefore, we compared IL-22 producing ILC3s in the intestinal lamina propria between *Dock8*$^{+/-}$ and *Dock8*$^{-/-}$ mice. As a result, we found that the percentage of IL-22 producing ILC3s (Lin^{-}RORγt-GFP^{+}IL-22^{+}) and their absolute number were markedly reduced in the intestinal lamina propria of *Dock8*$^{-/-}$ mice (Fig. 1D). Consistent with this, fucosylated epithelial cells (WGA^{+}UEA-1^{+}) were hardly

detected in the small intestine of *Dock8*$^{-/-}$ mice (Supplementary Figure 2). It is clear that IL-22 produced by ILC3s play an important role in fucosylation, because i.p. treatment of *Dock8*$^{-/-}$ mice with recombinant murine IL-22 induced fucosylation of intestinal epithelial cells (Supplementary Figure 2). Collectively, these results indicate that DOCK8 deficiency reduces the number of ILC3s in the small intestine and impairs IL-22-mediated cellular functions.

DOCK8 controls the number of intestinal ILC3s in a cell-autonomous manner

To examine whether DOCK8 expression in ILC3s is required to maintain the number of ILC3s in the small intestine, we crossed the gene-targeted mice harboring *loxP*-flanked exon3 of *Dock8* allele (*Dock8*$^{lox/lox}$ mice) with *Rorc-Cre mice* (29, 30). Although it is known that CD4^{+}CD8^{+} double-positive thymocytes express RORγt transiently (38, 39), *Dock8* expression was detected in intestinal T cells of *Rorc-Cre Dock8*$^{lox/lox}$ mice (Fig. 2A). Similar results were obtained when BM neutrophils and splenic B cells were analyzed (Fig. 2A). However, DOCK8 expression was completely deleted in intestinal ILC3s from *Rorc-Cre Dock8*$^{lox/lox}$ mice (Fig. 2A). By crossing *Rorc-Cre Dock8*$^{lox/lox}$ mice with RORγt-GFP mice, we found that genetic deletion of *Dock8* in RORγt^{+}-lineage cells markedly reduced not only the percentage, but also the number of NKp46^{+} ILC3s and CD4^{+} ILC3s (Fig. 2B), as seen in conventional *Dock8*$^{-/-}$ mice (see Fig. 1B). In contrast, the percentage of NKp46^{+} ILC3s and CD4^{+} ILC3s in total Lin^{-} populations and their absolute numbers were unchanged between *CD11c (Itgax)-Cre Dock8*$^{lox/+}$ and *Dock8*$^{lox/lox}$ mice (Supplementary Figure 3). We also found that the percentage and the number of IL-22 producing ILC3s was significantly reduced in *Rorc-Cre Dock8*$^{lox/lox}$ mice (Fig. 2C). In line with this, fucosylated epithelial cells were hardly

detected in the small intestine of *Rorc-Cre Dock8*$^{lox/lox}$ mice (Supplementary Figure 4). Thus, DOCK8 controls the number of intestinal ILC3s in a cell-autonomous manner.

DOCK8 expression is not required for differentiation into ILC3s

ILC3s can be differentiated in the presence of SCF and IL-7 *in vitro* from the lineage-negative (Lin$^-$) $\alpha4\beta7^+$ CD127$^+$ common helper innate lymphoid cell progenitors (CHILPs) in fetal liver (34, 40). To determine how DOCK8 controls the number of ILC3s, we first compared differentiation into ILC3s between *Dock8*$^{+/-}$ and *Dock8*$^{-/-}$ mice. The expressions of c-Kit (a receptor for SCF) and CD127 (IL-7Rα) on Lin$^-$RORγt-GFP$^+$ ILC3s were unchanged between *Dock8*$^{+/-}$ and *Dock8*$^{-/-}$ mice (Fig. 3A). In addition, we found that irrespective of the expression of DOCK8, the CHILPs in fetal liver normally differentiated into RORγt$^+$ ILC3s when cultured with OP9 stromal cells in the presence of SCF and IL-7 *in vitro* for 7 days, although the majority of differentiated ILC3s were NKp46$^-$CD4$^-$ (Fig. 3B and C). These results indicate that DOCK8 is dispensable for ILC3 differentiation.

DOCK8 regulates survival of ILC3s through Cdc42 activation

We then examined whether DOCK8 deficiency affects proliferation of ILC3s *in vivo*. For this purpose, we labelled ILC3s with BrdU and measured its incorporation by flow cytometry. We found that ILC3s from both *Dock8*$^{+/-}$ and *Dock8*$^{-/-}$ mice comparably incorporated BrdU (Fig. 4A), suggesting that DOCK8 deficiency does not affect proliferation of ILC3s. However, *in vitro* apoptosis assay revealed that under the condition with or without IL-7, the percentage of Annexin V$^+$ cells increased more than 2-fold in the case of *Dock8*$^{-/-}$ ILC3s, compared with

Dock8$^{+/-}$ controls (Fig. 4B). These results indicate that DOCK8 expression is required for survival of ILC3s.

Having found that DOCK8 regulates survival of ILC3s, we next examined whether this function of DOCK8 is mediated through the GEF activity for Cdc42. By analogy of the DOCK9-DHR2 domain, the valine residue at position 1986 of DOCK8 was expected to function as nucleotide sensor (41). Indeed, biochemical analyses revealed that the Cdc42 GEF activity of the recombinant DOCK8 DHR2 protein was completely abolished by mutating this valine residue to alanine (VA mutation), despite the quality of purified proteins being unaffected (Fig. 5A and B). Similarly, the Cdc42 GEF activity was also lost when glycine at position 1980 was mutated to arginine (GR mutation) (Fig. 5A and B). Although wild-type DOCK8 activated Cdc42 following overexpression in HEK-293T cells, Cdc42 activation was not induced in the case of DOCK8 having either VA mutation or GR mutation or both of them (VAGR mutation) (Fig. 5C).

This finding led us to examine how bi-allelic VAGR mutation of DOCK8 affects ILC3 population in the small intestine. For this purpose, we generated C57BL/6J mice having bi-allelic VAGR mutations (*Dock8*^{VAGR}) using CRISPR/Cas9-mediated genome editing system (Supplementary Figure 1). By crossing these mice with RORγt-GFP mice, we found that the percentages of both NKp46^{+} ILC3s and CD4^{+} ILC3s in total Lin^{-} populations and their absolute numbers were markedly reduced in the intestinal lamina propria of *Dock8*^{VAGR} mice (Fig. 6A). In addition, the percentage and the number of IL-22 producing ILC3s were also reduced in these mice (Fig. 6B). Importantly, ILC3s isolated from *Dock8*^{VAGR} mice showed increased susceptibility to cell apoptosis under the condition with or without

IL-7 (Fig. 6C). These results indicate that DOCK8 regulates survival of ILC3s in the gut through Cdc42 activation.

Discussion

Although *N*-ethyl-*N*-nitrosourea–mediated mutagenesis in mice has shown that DOCK8 mutations cause a reduction of RORγt$^+$ ILC3s in the small intestine (28), the underlying mechanism is not completely understood. By using DOCK8 conditional KO mice and *Dock8*^{VAGR} knock-in mutant mice, we have demonstrated that DOCK8 acts in ILC3 itself and regulates their survival through Cdc42 activation.

So far, it has been reported that DOCK8-deficient hematopoietic progenitor cells fail to give rise to RORγt$^+$ ILC3s, by analyzing the chimeric mice reconstituted with equal numbers of WT and DOCK8-deficient BM cells (28). Although this study indicated the importance of DOCK8 in hematopoietic cells, it remains unknown which types of hematopoietic cells require DOCK8 expression. This is the issue of physiological relevance, because recent evidence indicates that DCs indirectly control the number and the function of ILC3s in the small intestine (42, 43). In this study, we have shown that the percentage and the number of RORγt$^+$ ILC3s were unchanged between *CD11c (Itgax)-Cre Dock8*$^{lox/+}$ and *Dock8*$^{lox/lox}$ mice. In contrast, *Rorc-Cre Dock8*$^{lox/lox}$ mice as well as conventional *Dock8*$^{-/-}$ mice exhibited a severe reduction of ILC3s with increased susceptibility to apoptosis. These results suggest that DOCK8 expression in ILC3s is required to protect them from apoptosis.

DOCK8 is a Cdc42-specific GEF, but GEF-independent functions have been also reported for DOCK8 in antigen-induced IL-31 production in helper T cells (44). To examine whether DOCK8 functions as a Cdc42 GEF in this context, we generated *Dock8*^{VAGR} mice and found that RORγt$^+$ ILC3s were markedly reduced in

the small intestine with increased susceptibility to apoptosis. Although a previous study has suggested that DOCK8 mutations impair IL-7 receptor signaling (28), DOCK8 deficiency increased susceptibility to apoptosis under the condition with or without IL-7. It is currently unknown how DOCK8-Cdc42 axis regulates survival of ILC3s. This is an important question that should be investigated in future studies.

In conclusion, we have demonstrated that DOCK8 acts in cell-autonomous manner to control survival of ILC3s in the gut through Cdc42 activation. *Dock8*^{VAGR} mice would be a useful tool to distinguish between GEF-dependent and -independent functions of DOCK8.

Funding

This work was supported by the Japan Agency for Medical Research and Development (grant JP19gm0010001, JP20gm1310005 and JP20ek0410064 to Y.F.).

Acknowledgements

We thank Drs. Shinichiro Sawa (Kyushu University) and Gérard Eberl (Institut Pasteur, Paris, France) for providing us genetically engineered mice (RORγt-GFP Tg and *Rorc-Cre* Tg mice). We also thank Ayumi Inayoshi, Arisa Aosaka, Sayaka Akiyoshi, Satomi Hori, and Nao Kanematsu for technical assistance.

Conflicts of interest statement: the authors declared no conflicts of interest.

References

1. Spits, H. and Di Santo, J. P. 2011. The expanding family of innate lymphoid cells: regulators and effectors of immunity and tissue remodeling. *Nat. Immunol.* 12:21.

2. Eberl, G., Colonna, M., Di Santo, J. P. and McKenzie, A. N. J. 2015. Innate lymphoid cells: A new paradigm in immunology. *Science* 348:aaa6566.

3. Spits, H., Artis, D., Colonna, M. *et al.* 2013. Innate lymphoid cells — a proposal for uniform nomenclature. *Nat. Rev. Immunol.* 13:145.

4. Cella, M., Fuchs, A., Vermi, W. *et al.* 2009. A human natural killer cell subset provides an innate source of IL-22 for mucosal immunity. *Nature* 457:722.

5. Satoh-Takayama, N. 2015. Heterogeneity and diversity of group 3 innate lymphoid cells: new cells on the block. *Int. Immunol.* 28:29.

6. Buettner, M. and Lochner, M. 2016. Development and Function of Secondary and Tertiary Lymphoid Organs in the Small Intestine and the Colon. *Front. Immunol.* 7:342.

7. Robinette, M. L., Fuchs, A., Cortez, V. S. *et al.*; The Immunological Genome Consortium. 2015. Transcriptional programs define molecular characteristics of innate lymphoid cell classes and subsets. *Nat. Immunol.* 16:306.

8. Zhong, C., Zheng, M. and Zhu, J. 2018. Lymphoid tissue inducer—A divergent member of the ILC family. *Cytokine Growth Factor Rev.* 42:5.

9. Heasman, S. J. and Ridley, A. J. 2008. Mammalian Rho GTPases: new insights into their functions from in vivo studies. *Nat. Rev. Mol. Cell Biol.* 9:690.

10. Melendez, J., Grogg, M. and Zheng, Y. 2011. Signaling Role of Cdc42 in Regulating Mammalian Physiology. *J. Biol. Chem.* 286:2375.

11. Lämmermann, T., Renkawitz, J., Wu, X. Hirsch, K., Brakebusch, C. and Sixt, M. 2009. Cdc42-dependent leading edge coordination is essential for interstitial

dendritic cell migration. *Blood* 113:5703.

12. Lee, K., Boyd, K. L., Parekh, D. V. *et al.* 2013. Cdc42 Promotes Host Defenses against Fatal Infection. *Infect. Immun.* 81:2714.

13. Guo, F., Velu, C. S., Grimes, H. L. and Zheng, Y. 2009. Rho GTPase Cdc42 is essential for B-lymphocyte development and activation. *Blood* 114:2909.

14. Guo, F., Hildeman, D., Tripathi, P., Velu, C. S., Grimes, H. L. and Zheng, Y. 2010. Coordination of IL-7 receptor and T-cell receptor signaling by cell-division cycle 42 in T-cell homeostasis. *Proc. Natl. Acad. Sci. USA* 107:18505.

15. Kunimura, K., Uruno, T. and Fukui, Y. 2020. DOCK family proteins: key players in immune surveillance mechanisms. *Int. Immunol.* 32:5.

16. Harada, Y., Tanaka, Y., Terasawa, M. *et al.* 2012. DOCK8 is a Cdc42 activator critical for interstitial dendritic cell migration during immune responses. *Blood* 119:4451.

17. Engelhardt, K. R., Gertz, M. E., Keles, S. *et al.* 2015. The extended clinical phenotype of 64 patients with dedicator of cytokinesis 8 deficiency. *J. Allergy Clin. Immunol.* 136:402.

18. Sanal, O., Jing, H., Ozgur, T. *et al.* 2012. Additional diverse findings expand the clinical presentation of DOCK8 deficiency. *J. Clin. Immunol.* 32:698.

19. Zhang, Q., Davis, J. C., Lamborn, I. T. *et al.* 2009. Combined Immunodeficiency Associated with *DOCK8* Mutations. *N. Engl. J. Med.* 361:2046.

20. Zhang, Q., Davis, J. C., Dove, C. G. and Su, H. C. 2010. Genetic, clinical, and laboratory markers for DOCK8 immunodeficiency syndrome. *Dis. Markers* 29:131.

21. Jabara, H. H., McDonald, D. R., Janssen, E. *et al.* 2012. DOCK8 functions as an adaptor that links TLR-MyD88 signaling to B cell activation. *Nat. Immunol.* 13:612.

22. Mizesko, M. C., Banerjee, P. P., Monaco-Shawver, L. *et al.* 2013. Defective actin

accumulation impairs human natural killer cell function in patients with dedicator of cytokinesis 8 deficiency. *J. Allergy Clin. Immunol.* 131:840.

23. Randall, K. L., Chan, S. S.-Y. and Ma, C. S. 2011. DOCK8 deficiency impairs CD8 T cell survival and function in humans and mice. *J. Exp. Med.* 208:2305.

24. Zhang, Q., Dove, C. G., Hor, J. L. *et al.* 2014. DOCK8 regulates lymphocyte shape integrity for skin antiviral immunity. *J. Exp. Med.* 211:2549.

25. Crawford, G., Enders, A., Gileadi, U. *et al.* 2013. DOCK8 is critical for the survival and function of NKT cells. *Blood* 122:2052.

26. Lambe, T., Crawford, G., Johnson, A. L. *et al.* 2011. DOCK8 is essential for T-cell survival and the maintenance of $CD8^+$ T-cell memory. *Eur. J. Immunol.* 41:3423.

27. Randall, K. L., Lambe, T., Johnson, A. L. *et al.* 2009. Dock8 mutations cripple B cell immunological synapses, germinal centers and long-lived antibody production. *Nat. Immunol.* 10:1283.

28. Singh, A. K., Eken, A., Fry, M., Bettelli, E. and Oukka, M. 2014. DOCK8 regulates protective immunity by controlling the function and survival of $ROR\gamma t^+$ ILCs. *Nat. Commun.* 5:4603.

29. Kunimura, K., Sakata, D., Tun, X. *et al.* 2019. S100A4 Protein Is Essential for the Development of Mature Microfold Cells in Peyer's Patches. *Cell Rep.* 29:2823.

30. Sawa, S., Cherrier, M., Lochner, M. *et al.* 2010. Lineage Relationship Analysis of $ROR\gamma t^+$ Innate Lymphoid Cells. *Science* 330:665.

31. Caton, M. L., Smith-Raska, M. R. and Reizis, B. 2007. Notch-RBP-J signaling controls the homeostasis of $CD8^-$ dendritic cells in the spleen. *J. Exp. Med.* 204:1653.

32. Emgård, J., Kammoun, H., García-Cassani, B. *et al.* 2018. Oxysterol Sensing

through the Receptor GPR183 Promotes the Lymphoid-Tissue-Inducing Function of Innate Lymphoid Cells and Colonic Inflammation. *Immunity* 48:120

33. Goto, Y., Obata, T., Kunisawa, J. *et al.* 2014. Innate lymphoid cells regulate intestinal epithelial cell glycosylation. *Science* 345:1254009.

34. Klose, C. S. N., Flach, M., Möhle, L. *et al.* 2014. Differentiation of Type 1 ILCs from a Common Progenitor to All Helper-like Innate Lymphoid Cell Lineages. *Cell* 157:340.

35. Liu, B., Ye, B., Yang, L. *et al.* 2017. Long noncoding RNA lncKdm2b is required for ILC3 maintenance by initiation of Zfp292 expression. *Nat. Immunol.* 18:499.

36. Bostick, J. W., Wang, Y., Shen, Z. *et al.* 2019. Dichotomous regulation of group 3 innate lymphoid cells by nongastric *Helicobacter* species. *Proc. Natl. Acad. Sci. USA* 116:24760.

37. Shiraishi, A., Uruno, T., Sanematsu, F. *et al.* 2017. DOCK8 Protein Regulates Macrophage Migration through Cdc42 Protein Activation and LRAP35a Protein Interaction. *J. Biol. Chem.* 292:2191.

38. He, Y. W., Deftos, M. L., Ojala, E. W. and Bevan, M. J. 1998. RORγt, a Novel Isoform of an Orphan Receptor, Negatively Regulates Fas Ligand Expression and IL-2 Production in T Cells. *Immunity* 9:797.

39. He, Y. W., Beers, C., Deftos, M. L., Ojala, E. W., Forbush, K. A. and Bevan, M.J., 2000. Down-Regulation of the Orphan Nuclear Receptor RORγt Is Essential for T Lymphocyte Maturation. *J. Immunol.* 164:5668.

40. van de Pavert, S. A. and Vivier, E. 2015. Differentiation and function of group 3 innate lymphoid cells, from embryo to adult. *Int. Immunol.* 28:35.

41. Yang, J., Zhang, Z., Roe, S. M., Marshall, C. J. and Barford, D. 2009. Activation of Rho GTPases by DOCK exchange factors is mediated by a nucleotide sensor.

Science 325:1398.

42. Bernink, J. H., Krabbendam, L., Germar, K. *et al.* 2015. Interleukin-12 and -23 Control Plasticity of CD127^{+} Group 1 and Group 3 Innate Lymphoid Cells in the Intestinal Lamina Propria. *Immunity* 43:146.

43. Longman, R. S., Diehl, G. E., Victorio, D. A. *et al.* 2014. CX3CR1^{+} mononuclear phagocytes support colitis-associated innate lymphoid cell production of IL-22. *J. Exp. Med.* 211:1571.

44. Yamamura, K., Uruno, T., Shiraishi, A. *et al.* 2017. The transcription factor EPAS1 links DOCK8 deficiency to atopic skin inflammation via IL-31 induction. *Nat. Commun.* 8:13946.

Main figure titles and legends

Fig. 1. DOCK8 deficiency reduces ILC3s in the small intestine. (A, B) Flow cytometric analyses for NKp46-ILC3s (RORγt$^+$NKp46$^+$) and CD4-ILC3s (RORγt$^+$CD4$^+$) in the intestinal lamina propria from *Dock8*$^{+/-}$ and *Dock8*$^{-/-}$ mice in the absence (A) or presence (B) of RORγt-GFP transgene. The percentage (middle panels) of NKp46-ILC3s and CD4-ILC3s to the total Lin$^-$ cells and their absolute numbers (right panels) were compared between them (n = 5). (C) Representative sections of the small intestine from *Dock8*$^{+/-}$ and *Dock8*$^{-/-}$ RORγt-GFP mice (left panel). In the right panel, the total number of CPs and ILFs in 20 sections are compared between *Dock8*$^{+/-}$ and *Dock8*$^{-/-}$ RORγt-GFP mice (n = 5). Arrows or arrowheads indicate CPs (RORγt$^+$B220$^-$ clusters) or ILFs (RORγt$^+$B220$^+$ clusters), respectively. Higher magnifications of the indicated area are shown at the corner. Scale bars, 250 μm. (D) Flow cytometric analyses for IL-22 producing ILC3s in the intestinal lamina propria from *Dock8*$^{+/-}$ and *Dock8*$^{-/-}$ RORγt-GFP mice. The percentage (left panel) of IL-22 producing ILC3s to the total Lin$^-$ cells and their absolute numbers (right panels) were compared between them (n = 5). IL-22 expression in ILC3s (Lin$^-$RORγt-GFP$^+$) was analyzed by intracellular cytokine staining, after stimulated with PMA and ionomycin calcium salt at 37°C for 4 h in the presence of brefeldin A. In (A)–(D), data are expressed as mean ± SD. $^{**}P < 0.01$; $^{***}P < 0.005$ by two-tailed unpaired Student's *t*-test.

Fig. 2. DOCK8 controls the number of intestinal ILC3s in a cell-autonomous manner. (A) Reverse transcription-PCR analysis for the expression of *Dock8* and *Gapdh*. Intestinal ILC3s, intestinal T cells, splenic B cells and BM neutrophils were sorted from *Rorc-Cre Dock8*$^{lox/+}$ and *Dock8*$^{lox/lox}$ mice. Amplification increased by 3 cycles,

from the left to the right, starting at 30 cycles for *Gapdh* or 33 cycles for *Dock8*. Data are representative of two independent experiments. (B) Flow cytometric analyses for NKp46-ILC3s (RORγt-GFP$^+$NKp46$^+$) and CD4-ILC3s (RORγt-GFP$^+$CD4$^+$) in the intestinal lamina propria from *Rorc-Cre Dock8$^{lox/+}$* and *Dock8$^{lox/lox}$* mice expressing RORγt-GFP transgene. The percentage (middle panels) of NKp46-ILC3s and CD4-ILC3s to the total Lin$^-$ cells and their absolute numbers (right panels) were compared between them (n = 5). (C) Flow cytometric analyses for IL-22 producing ILC3s in the intestinal lamina propria from *Rorc-Cre Dock8$^{lox/+}$* and *Dock8$^{lox/lox}$* mice expressing RORγt-GFP transgene. The percentage (middle panel) of IL-22 producing ILC3s to the total Lin$^-$ cells and their absolute numbers (right panels) were compared between them (n = 5). In (B) and (C), data are expressed as mean ± SD. $^{**}P < 0.01$; $^{***}P < 0.005$ by two-tailed unpaired Student's *t*-test.

Fig. 3. DOCK8 deficiency dose not affect the expression of c-Kit/CD127 and the differentiation of ILC3s. (A) Histogram (left panel) and the frequency (right panel) of c-Kit (SCF receptor) and CD127 (IL-7Rα) expression on Lin$^-$RORγt-GFP$^+$ ILC3s in the intestinal lamina propria are compared between *Dock8$^{+/-}$* and *Dock8$^{-/-}$* RORγt-GFP mice (n = 5). (B) Schematic representation of in vitro differentiation system used in this study. (C) Flow cytometric analyses for RORγt$^+$ ILC3s differentiated from CHILPs in *Dock8$^{+/-}$* and *Dock8$^{-/-}$* fetal liver cells expressing RORγt-GFP transgene. The percentage of NKp46$^+$ ILC3s and CD4$^+$ ILC3s (middle panels) and the percentage of NKp46$^-$ ILC3s and CD4$^-$ ILC3s (right panels) to the total Lin$^-$ cells were compared between them (n = 3). Data are expressed as mean ± SD. ns, not significant by two-tailed unpaired Student's *t*-test (A) and two-tailed Mann-Whitney test (C).

Fig. 4. DOCK8 deficiency impairs survival, but not proliferation of ILC3s. (A) Flow cytometric plot (left panel) and the percentage (right panel) of $BrdU^+$ ILC3s to the total $Lin^-ROR\gamma t\text{-}GFP^+$ cells in the intestinal lamina propria (n = 5). *Dock8*$^{+/-}$ and *Dock8*$^{-/-}$ RORγt-GFP mice were injected i.p. with BrdU (200 μg) and murine IL-23 (1 μg), and then fed continuously with water containing 800 μg ml^{-1} BrdU and 5% glucose for 16 h. (B) Flow cytometric plot (left panel) and the percentage (right panel) of Annexin V^+ ILC3s to the total $Lin^-ROR\gamma t\text{-}GFP^+$ cells (n = 5). $Lin^-ROR\gamma t\text{-}GFP^+$ ILC3s were sorted into 96-well plates from intestinal lamina propria from *Dock8*$^{+/-}$ and *Dock8*$^{-/-}$ RORγt-GFP mice. After incubation for 18 h with or without 25 ng ml^{-1} murine IL-7, cell apoptosis was assessed by Annexin V staining. In (A) and (B), data are expressed as mean ± SD. $^{**}P < 0.01$; $^{***}P < 0.005$; ns, not significant by two-tailed unpaired Student's *t*-test.

Fig. 5. VA and GR mutations in DOCK8-DHR2 domain fail to activate Cdc42. (A) Proteins used for the assay. His-SUMO-tagged DOCK8-DHR2 domain (5 μg each, wild-type (WT), VA, GR, and VAGR mutant) were separated on a 10% SDS-polyacrylamide gel and stained with Coomassie Brilliant Blue. The position and size of the molecular weight markers are indicated in the left side. Data are representative of two independent experiments. (B) Time course of fluorescent GEF assays. His-SUMO-tagged recombinant WT or mutant (VA, GR, and VAGR) DOCK8-DHR2 proteins (residues 1633–2071) at final concentrations of 62.5–1000 nM were analyzed for their GEF activities toward Cdc42 using BODIPY-FL-GTP. RFU, relative fluorescence units. Data are representative of two independent experiments. (C) Following overexpression of the indicated constructs in HEK-293T

cells, activation of Cdc42 was analysed. Cell lysates were subjected to pull-down assays using the GST-fusion Cdc42-binding domain of PAK1 before immunoblotting with anti-Cdc42 antibody. Data are representative of two independent experiments.

Fig. 6. DOCK8 regulates survival of ILC3s through Cdc42 activation. (A) Flow cytometric analyses for NKp46-ILC3s (RORγt$^+$NKp46$^+$) and CD4-ILC3s (RORγt$^+$CD4$^+$) in the intestinal lamina propria from *Dock8*$^{+/+}$ and *Dock8*^{VAGR} RORγt-GFP mice. The percentage (middle panels) of NKp46-ILC3s and CD4-ILC3s to the total Lin$^-$ cells and their absolute numbers (right panels) were compared between them (n = 5). (B) Flow cytometric analyses for IL-22 producing ILC3s in the intestinal lamina propria from *Dock8*$^{+/+}$ and *Dock8*^{VAGR} RORγt-GFP mice. The percentage (middle panel) of IL-22 producing ILC3s to the total Lin$^-$ cells and their absolute numbers (right panels) were compared between them (n = 5). (C) Flow cytometric plot (left panel) and the percentage (right panel) of Annexin V$^+$ ILC3s to the total Lin$^-$RORγt-GFP$^+$ cells (n = 5). Lin$^-$RORγt-GFP$^+$ ILC3s were sorted into 96-well plates from intestinal lamina propria from *Dock8*$^{+/+}$ and *Dock8*^{VAGR} RORγt-GFP mice. After incubation for 18 h with or without 25 ng ml^{-1} murine IL-7, cell apoptosis was assessed by Annexin V staining. In (A)–(C), data are expressed as mean ± SD. $^{**}P < 0.01$; $^{***}P < 0.005$; ns, not significant by two-tailed unpaired Student's *t*-test.

Supplementary Fig. 1. A schematic illustration demonstrating the locations of the guide RNAs (gRNA) and ssODN along with the mouse *Dock8* locus. The deduced amino acid sequences from wild type and substituted sequences are shown. Blue

and red letters indicate the VA and GR substitution target sites in the *Dock8* locus, respectively. The orange bars and letters indicate the position of gRNA targets.

Supplementary Fig. 2. DOCK8 deficiency impairs epithelial fucosylation in the ileum. *Dock8*$^{+/-}$ and *Dock8*$^{-/-}$ mice were treated i.p. with recombinant murine IL-22 (1 μg) or PBS as a control one day before analysis. Whole-mount staining of the ileum was performed with UEA-1 (red) for α-1,2 fucose staining and WGA (green) for epithelial cell counterstaining. Data are representative of four independent experiments. Scale bars, 200 μm.

Supplementary Fig. 3. Genetic deletion of *Dock8* in CD11c^{+} cells does not affect the number of intestinal ILC3s. Flow cytometric analyses for NKp46-ILC3s (RORγt^{+}NKp46^{+}) and CD4-ILC3s (RORγt^{+}CD4^{+}) in the intestinal lamina propria from *CD11c (Itgax)-Cre Dock8*$^{lox/+}$ and *Dock8*$^{lox/lox}$ mice. The percentage (middle panels) of NKp46-ILC3s and CD4-ILC3s to the total Lin^{-} cells and their absolute numbers (right panels) were compared between them (n = 5). Data are expressed as mean ± SD. ns, not significant by two-tailed unpaired Student's *t*-test.

Supplementary Fig. 4. Genetic deletion of *Dock8* in RORγt^{+}-lineage cells impairs epithelial fucosylation in the ileum. Whole-mount staining of the ileum from *Rorc-Cre Dock8*$^{lox/+}$ and *Dock8*$^{lox/lox}$ mice was performed with UEA-1 (red) for α-1,2 fucose staining and WGA (green) for epithelial cell counterstaining. Data are representative of three independent experiments. Scale bars, 200 μm.

Figure. 1

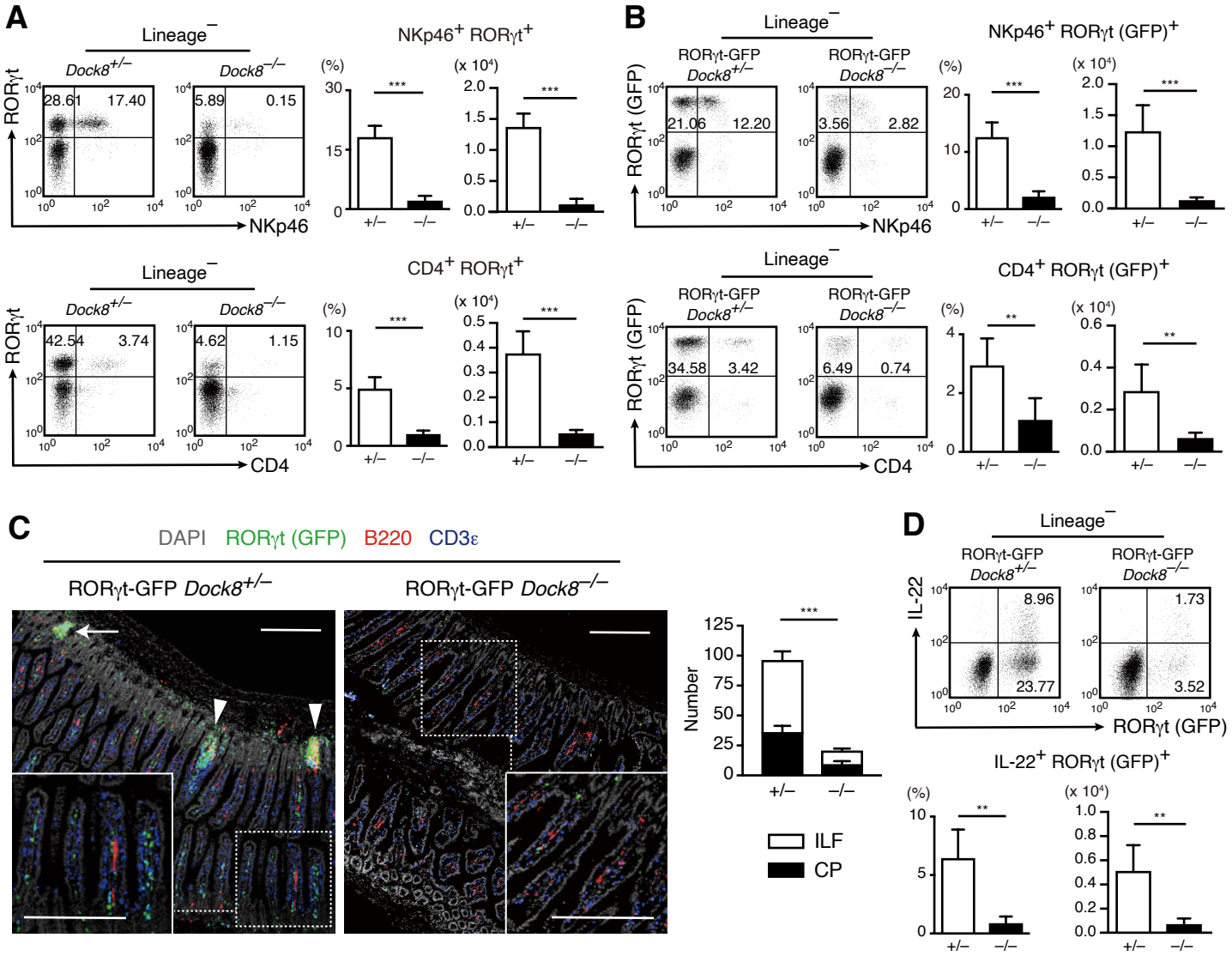
A
Lineage−
Dock8+/−
Dock8−/−
RORγt
NKp46
28.61
17.40
5.89
0.15
NKp46+ RORγt+
(%)
(x 10⁴)
***
+/−
−/−
CD4
42.54
3.74
4.62
1.15
CD4+ RORγt+
B
RORγt-GFP
RORγt (GFP)
21.06
12.20
3.56
2.82
NKp46+ RORγt (GFP)+
34.58
3.42
6.49
0.74
CD4+ RORγt (GFP)+
**
C
DAPI
RORγt (GFP)
B220
CD3ε
RORγt-GFP Dock8+/−
RORγt-GFP Dock8−/−
Number
ILF
CP
D
IL-22
8.96
23.77
1.73
3.52
IL-22+ RORγt (GFP)+

Figure. 2

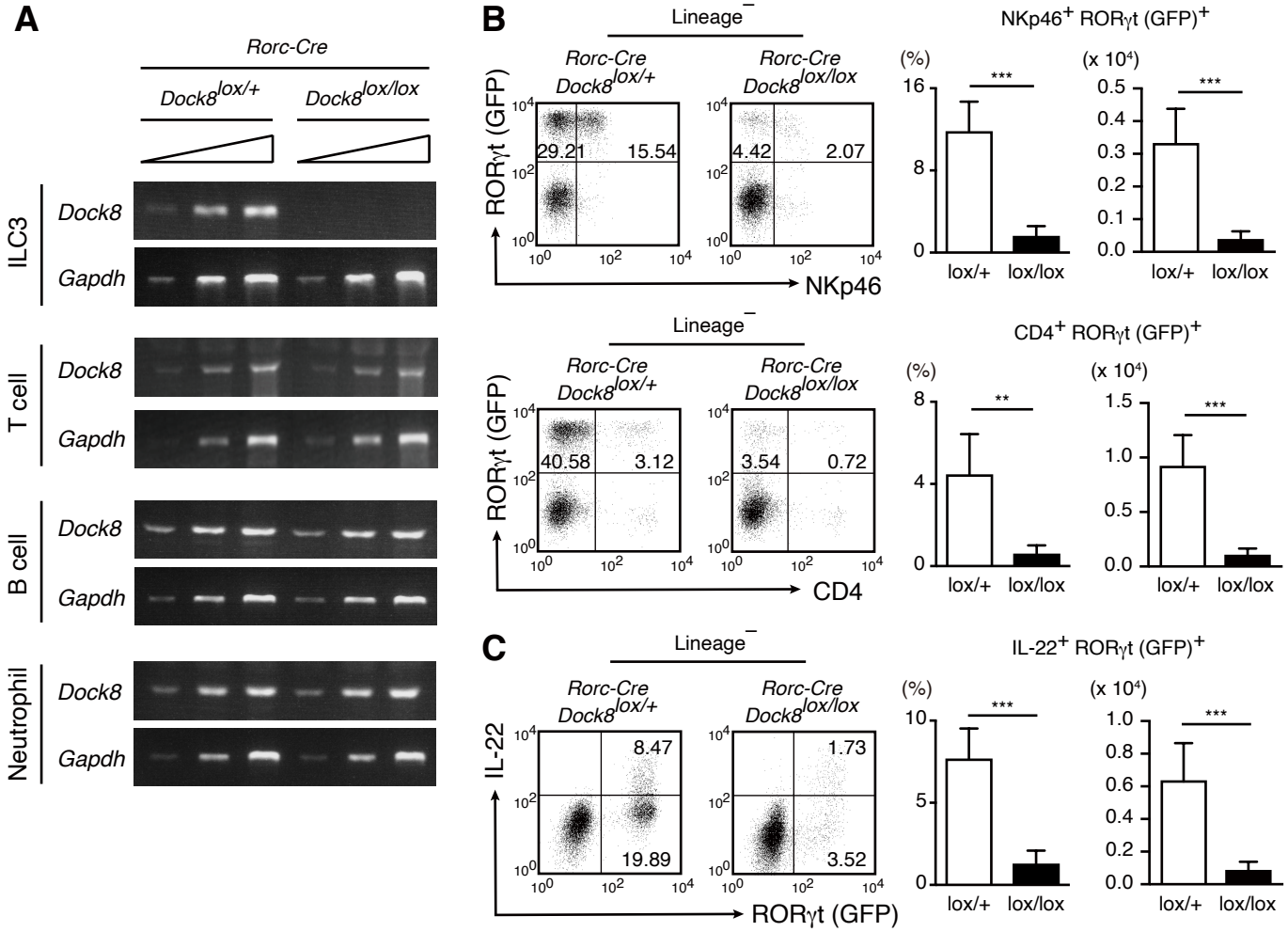
A
Rorc-Cre
Dock8lox/+
Dock8lox/lox
ILC3
T cell
B cell
Neutrophil
Dock8
Gapdh
B
Lineage−
Rorc-Cre Dock8lox/+
Rorc-Cre Dock8lox/lox
RORγt (GFP)
NKp46
29.21
15.54
4.42
2.07
NKp46+ RORγt (GFP)+
(%)
(x 10⁴)
lox/+
lox/lox
CD4
40.58
3.12
3.54
0.72
CD4+ RORγt (GFP)+
C
IL-22
8.47
19.89
1.73
3.52
IL-22+ RORγt (GFP)+

Figure. 3

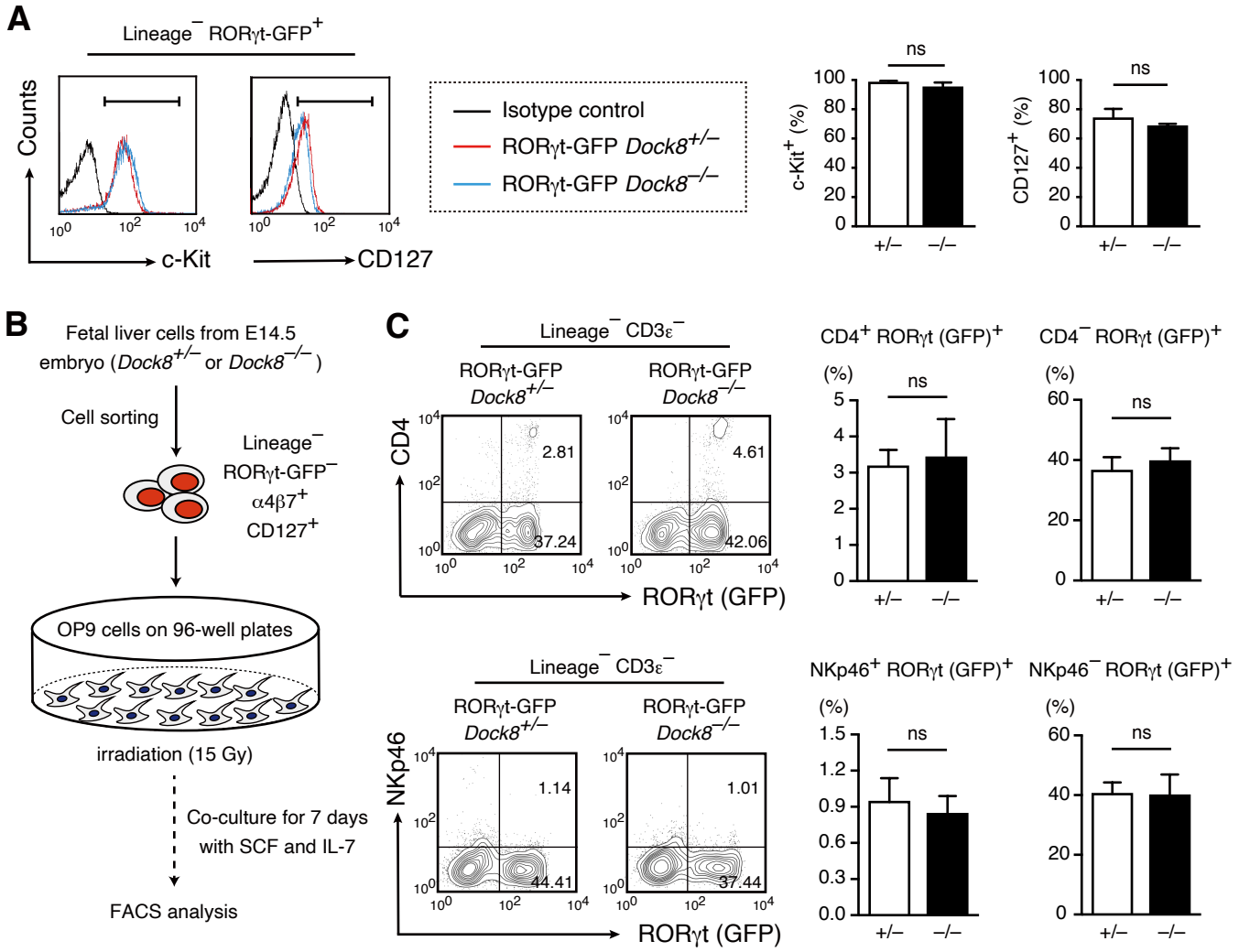
A
Lineage⁻ RORγt-GFP⁺
Counts
c-Kit
CD127
Isotype control
RORγt-GFP Dock8+/–
RORγt-GFP Dock8–/–
ns
c-Kit⁺ (%)
CD127⁺ (%)
+/–
–/–
B
Fetal liver cells from E14.5 embryo (Dock8+/– or Dock8–/–)
Cell sorting
Lineage⁻ RORγt-GFP⁻ α4β7⁺ CD127⁺
OP9 cells on 96-well plates
irradiation (15 Gy)
Co-culture for 7 days with SCF and IL-7
FACS analysis
C
Lineage⁻ CD3ε⁻
RORγt-GFP Dock8+/–
RORγt-GFP Dock8–/–
CD4
RORγt (GFP)
2.81
37.24
4.61
42.06
CD4⁺ RORγt (GFP)⁺
CD4⁻ RORγt (GFP)⁺
(%)
NKp46
1.14
44.41
1.01
37.44
NKp46⁺ RORγt (GFP)⁺
NKp46⁻ RORγt (GFP)⁺

Figure. 4

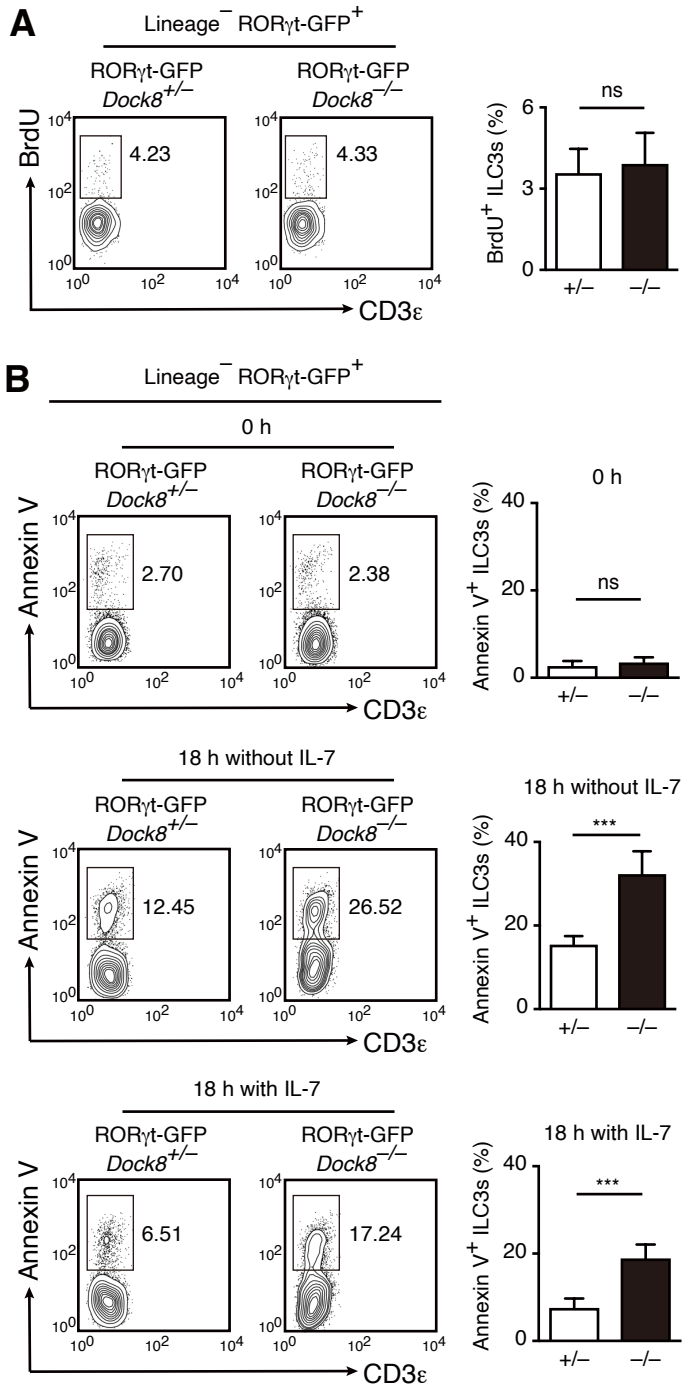
A
Lineage⁻ RORγt-GFP⁺
RORγt-GFP Dock8+/–
RORγt-GFP Dock8–/–
BrdU
4.23
4.33
CD3ε
ns
BrdU+ ILC3s (%)
+/–
–/–
B
Lineage⁻ RORγt-GFP⁺
0 h
Annexin V
2.70
2.38
Annexin V+ ILC3s (%)
18 h without IL-7
12.45
26.52
***
18 h with IL-7
6.51
17.24

Figure. 5

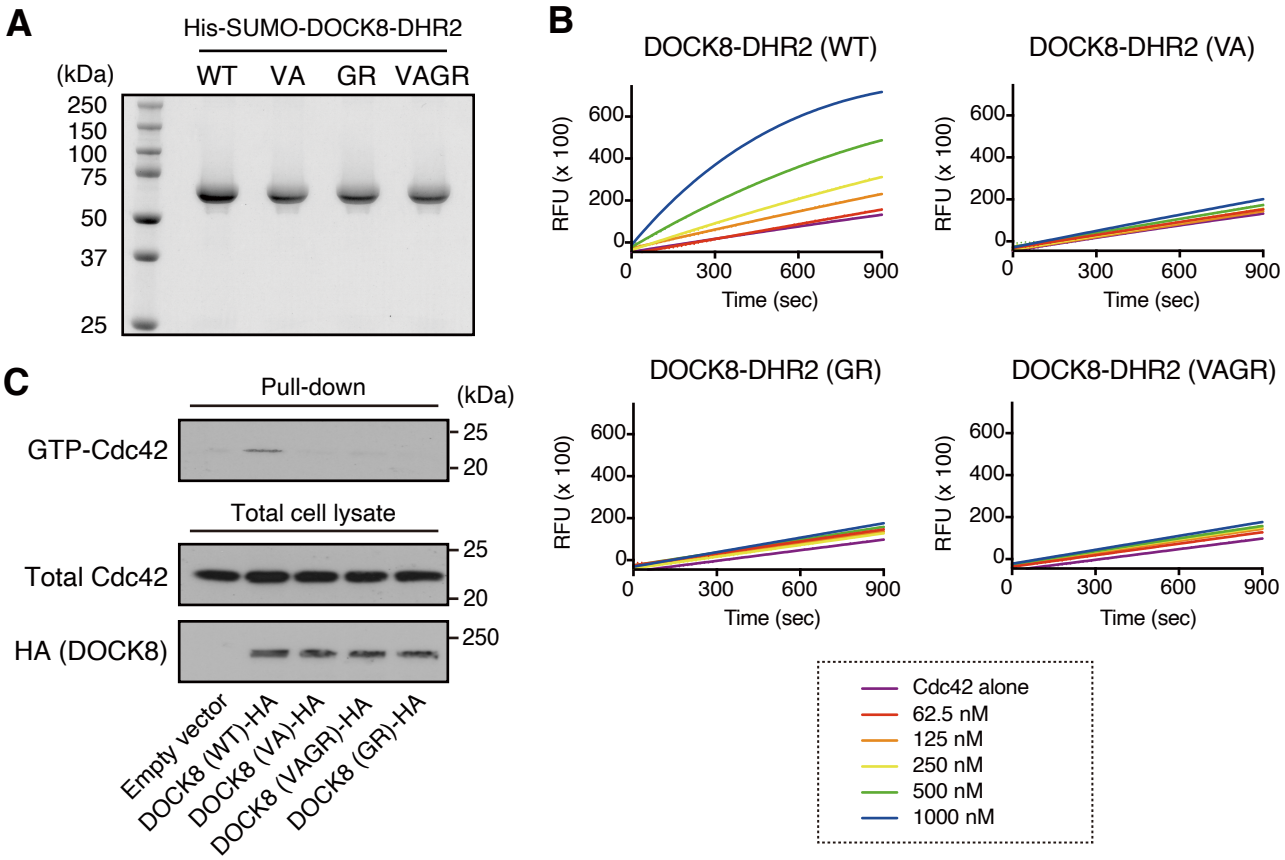
A
His-SUMO-DOCK8-DHR2
(kDa)
WT
VA
GR
VAGR
250
150
100
75
50
37
25
B
DOCK8-DHR2 (WT)
DOCK8-DHR2 (VA)
DOCK8-DHR2 (GR)
DOCK8-DHR2 (VAGR)
RFU (x 100)
Time (sec)
0
300
600
900
Cdc42 alone
62.5 nM
125 nM
250 nM
500 nM
1000 nM
C
Pull-down
(kDa)
GTP-Cdc42
Total cell lysate
Total Cdc42
HA (DOCK8)
25
20
250
Empty vector
DOCK8 (WT)-HA
DOCK8 (VA)-HA
DOCK8 (VAGR)-HA
DOCK8 (GR)-HA

Figure. 6

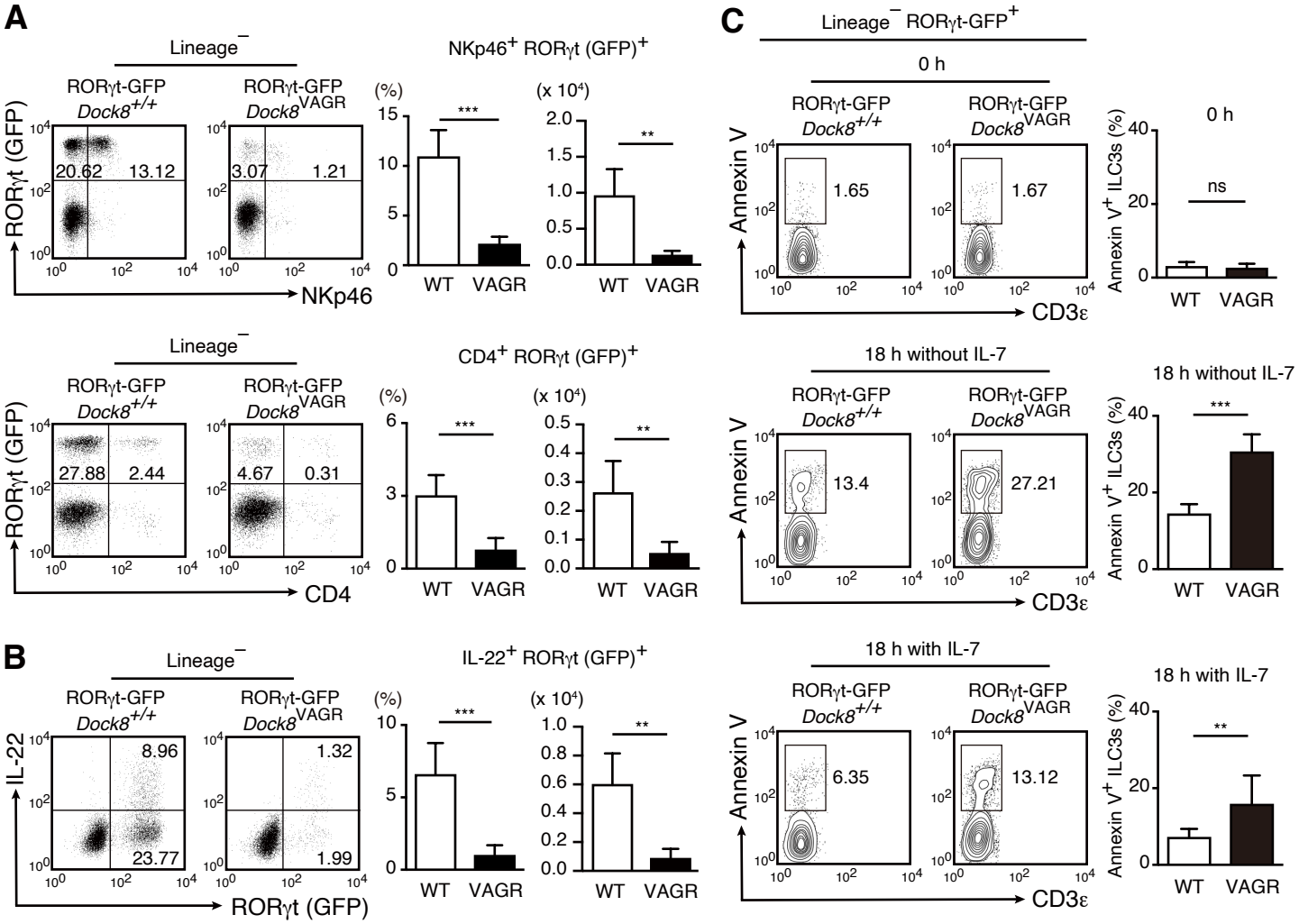
A
Lineage−
RORγt-GFP Dock8+/+
RORγt-GFP Dock8VAGR
RORγt (GFP)
NKp46
20.62
13.12
3.07
1.21
NKp46+ RORγt (GFP)+
(%)
(x 10⁴)
***
**
WT
VAGR
CD4
27.88
2.44
4.67
0.31
CD4+ RORγt (GFP)+
B
IL-22
8.96
23.77
1.32
1.99
IL-22+ RORγt (GFP)+
C
Lineage− RORγt-GFP+
0 h
Annexin V
CD3ε
1.65
1.67
Annexin V+ ILC3s (%)
ns
18 h without IL-7
13.4
27.21
18 h with IL-7
6.35
13.12

Supplementary Figure 1.

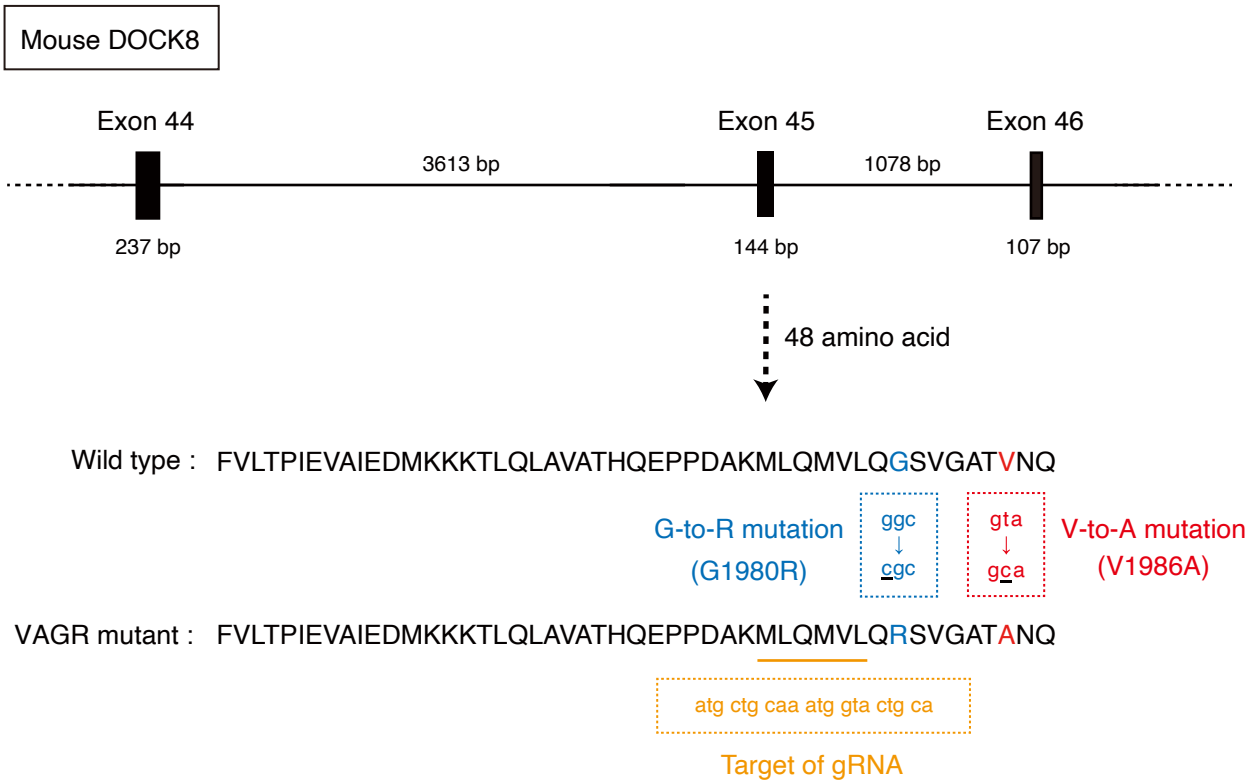

Supplementary Figure 2.

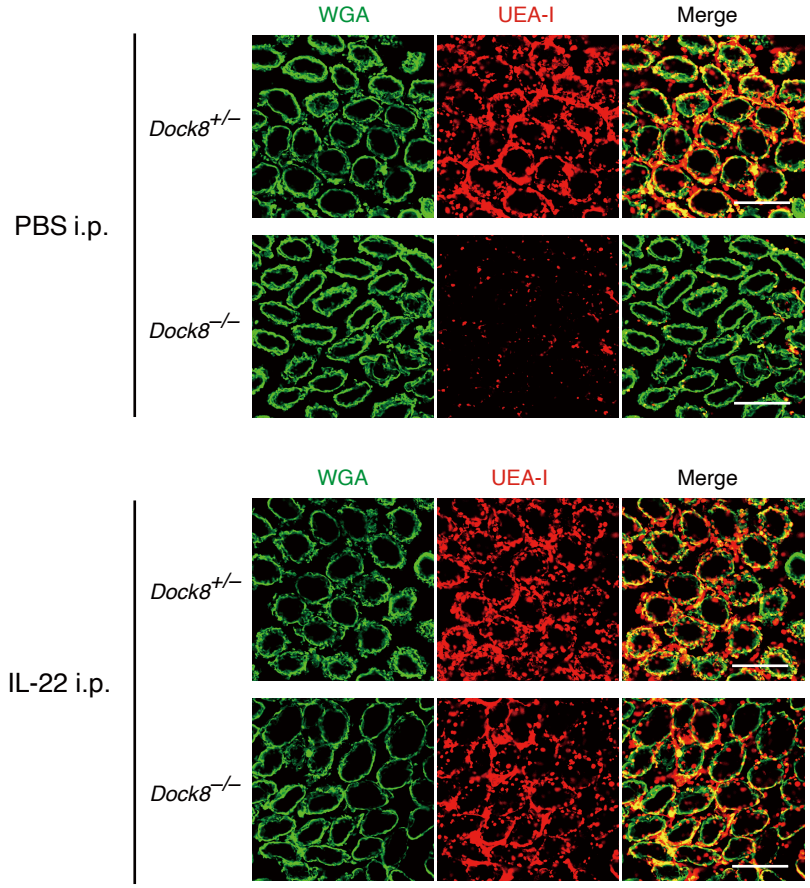

Supplementary Figure 3.

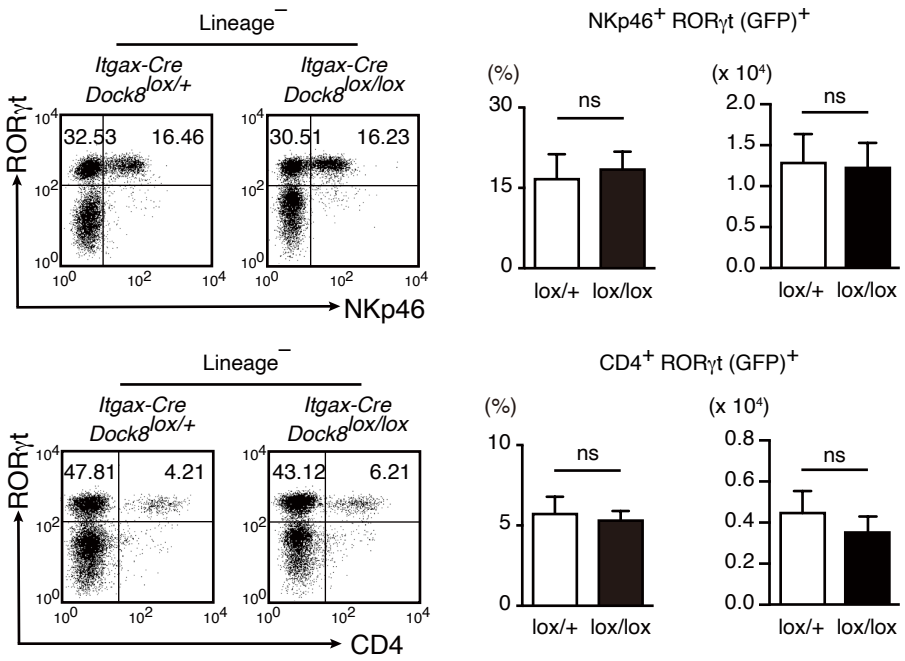
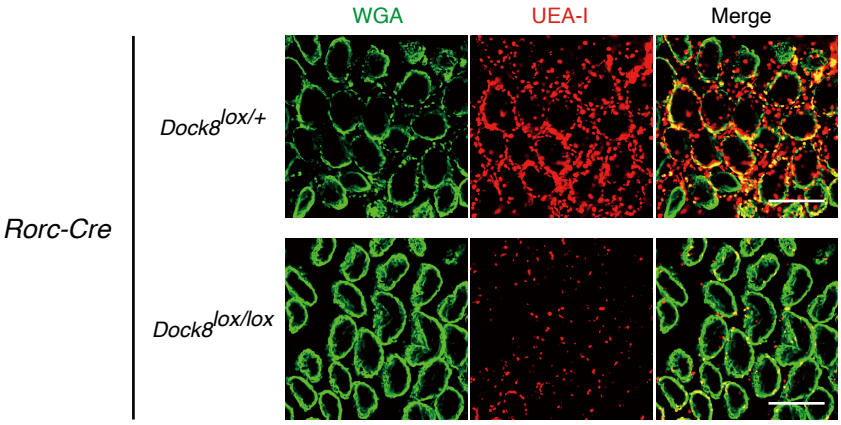
Supplementary Figure 4.